

Steady-state, cavity-less, multimode superradiance

Joel A. Greenberg and Daniel J. Gauthier

¹*Department of Physics and the Fitzpatrick Institute for Photonics, Duke University, Durham, NC 27708, USA*

The study of collective light-matter interactions, where the dynamics of an individual scatterer depend on the state of the entire multi-scatterer system, has recently received much attention in the areas of fundamental research and photonic technologies.^{1,2} Cold atomic vapors represent an exciting system for studying such effects because light-based manipulation of internal and center-of-mass atomic states lead to reduced instability thresholds^{3,4} and new phenomena. Previous investigations required single-mode cavities to realize strong light-mediated atom-atom interactions,⁵ though, which limits the observable phenomena.^{6,7} Here we demonstrate steady-state, mirrorless superradiance in a cold vapor pumped by weak optical fields. Beyond a critical pumping strength, the vapor spontaneously transforms into a spatially self-organized state: a density grating forms. Scattering of the pump beams off this grating generates new optical fields that act back on the vapor to enhance the atomic organization. This system has applications in many-body physics^{6,7} as well as quantum information processing.^{8,9}

One prominent example of collective behavior is superradiance,¹⁰ where light-induced couplings between initially incoherently-prepared emitters cause the full ensemble to synchronize and radiate coherently.¹¹ This leads to the emission of an intense pulse of light after a time delay τ_D ,

where τ_D corresponds to the time required for the atoms to synchronize. In order for this collective instability to occur, the system must possess sufficient gain and feedback so that synchronization occurs more rapidly than dephasing. While early studies of superradiance focused on collective scattering via the emitters' *internal* degrees of freedom, recent work demonstrates that formally identical behavior arises through the manipulation of *external* states of cold atoms.^{5,12,13}

In these studies, an initially uniformly-distributed gas of atoms pumped by external optical fields spontaneously undergoes a transition to a spatially-ordered state under certain circumstances.^{5,12-14} This ordering arises from the momentum imparted to the atoms via optical scattering and can be understood as a form of atomic synchronization: instead of the atoms scattering light individually, the self-assembled density grating enables the entire ensemble to coherently scatter light as a single entity. The pump beams scatter off this grating and produce new optical fields that act back on the vapor to enhance the grating contrast. This emergent, dynamical organization can lead to reduced optical instability thresholds³ and new phenomena⁶ that are inaccessible using static, externally-imposed optical lattices.⁴

In these processes, thermal atomic motion washes out the density grating and causes decoherence. Thus, previous observations of such instabilities in free space required ultracold temperatures ($T < 3 \mu\text{K}$) and employed optical fields detuned far from atomic resonance in order to avoid recoil-induced heating.^{14,15} Collective scattering in these systems is inherently transient, though, because the recoil associated with repeated scattering events eventually destroys the ultracold gas. By placing the atoms in a single-mode cavity, the enhanced duration of the light-matter interaction

effectively increases the coherence time and enables instabilities to occur at temperatures of up to $\sim 100 \mu\text{K}$. By including an auxiliary cooling mechanism, recent studies have demonstrated steady-state behavior.^{16,17} Nevertheless, single-mode cavities are more technically challenging to work with than free-space systems, impose additional constraints on the allowed optical frequencies, and are incompatible with multi-mode fields, which are necessary for realizing recently-proposed spin glass systems^{6,7,13} and multi-mode quantum information processing schemes.^{8,9}

In this Letter, we demonstrate a collective, superradiant instability that results in the steady-state emission of multi-mode optical fields in the absence of an optical cavity without requiring ultracold temperatures. To realize this instability, we use a magneto-optical trap (MOT) to produce an anisotropic, pencil-shaped cloud of cold ($T = 30 \mu\text{K}$) ^{87}Rb atoms.¹⁸ We then turn off the MOT beams and illuminate the atoms with a pair of weak, counterpropagating pump fields rotated by an angle $\theta = 10^\circ$ relative to the trap's long axis (see Fig. 1a). Unlike in previous studies, we work at small detunings Δ below atomic resonance (*i.e.*, several natural linewidths Γ) and choose the pump beam polarizations such that net cooling occurs via the Sisyphus effect.¹⁹

This configuration allows us to exploit a recently-reported gain mechanism in which atomic cooling enhances the loading of atoms into the optical lattice formed by the interference of the pump and self-generated optical fields.^{20,21} The pump fields scatter off this density grating and amplify the newly-produced, frequency degenerate optical fields. Atomic cooling in this compliant optical lattice results in typical atomic temperatures of a few μK , and the mutual amplification of the optical and density waves via this collective scattering mechanism results in the superradiant

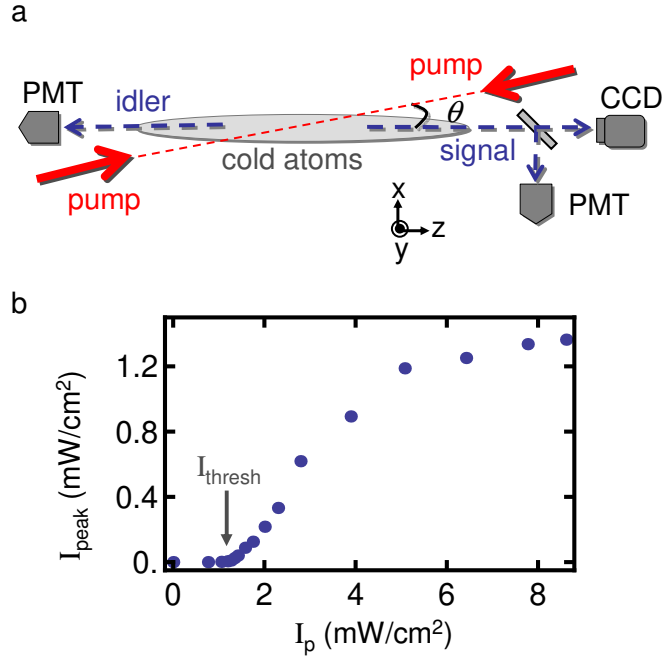


Figure 1: **Schematic of experimental setup and observation of superradiance threshold.** **a)** We apply a pair of weak, counterpropagating pump beams to a pencil-shaped cloud of cold atoms at an angle $\theta = 10^\circ$ relative to the \hat{z} axis. Scattering via the spontaneously-formed density grating produces signal and idler fields propagating along the trap's long axis. We use a pair of matched photomultiplier tubes (PMTs) and a charge-coupled device (CCD) camera to image the temporal and spatial profile of the generated light, respectively. **b)** Superradiance only occurs beyond a threshold pump intensity I_{thresh} . For a pump detuning $\Delta = -5 \pm 0.5 \Gamma$ and density $\eta = 5 \pm 2 \times 10^{10} \text{ cm}^{-3}$, we observe $I_{thresh} = 1.25 \pm 0.25 \text{ mW/cm}^2$, where I_p corresponds to the intensity of a single pump beam.

instability.^{13, 14, 22, 23}

Because the instability requires that the single-pass gain exceed the intrinsic system loss, superradiance only occurs when I_p exceeds a threshold pump intensity I_{thresh} (see Fig. 1b). This threshold intensity is typically a few mW/cm² and depends on Δ . The balance between efficient cooling at larger Δ and resonant enhancement at small Δ results in a minimum value of $I_{thresh} = 1 \pm 0.2$ mW/cm² for $\Delta = -3\Gamma$. This corresponds to a total input power of $P_{thresh} = 400 \pm 80$ μ W in our experiment, where we use pump beams with a 5 mm diameter and do not require any auxiliary beams to initially pre-condition the sample.^{4, 24} Beyond the instability threshold, the peak intensity of the generated light I_{peak} increases linearly with I_p before leveling off at $I_{peak} \sim 1$ mW/cm² near $I_p = 5$ mW/cm².

Mode competition leads to self-oscillation along the direction in which I_{thresh} is smallest. For our pencil-shaped MOT, we observe the emission of a pair of counterpropagating optical fields oriented along the vapor's long axis, which we refer to as signal and idler fields with intensities I_s and I_i , respectively. This counterpropagating geometry provides distributed feedback through the mutual coupling of the fields and also balances radiation pressure forces, which is necessary for continuous operation.¹⁶ Figure 2a shows the measured transverse intensity distribution of the signal beam $I_s(x, y)$ for two different MOT realizations. The generated light consists of multiple transverse spatial modes, which indicates the existence of atomic self-organization in all three dimensions. The interplay between mode competition and the random initial fluctuations that seed the instability cause $I_{s,i}(x, y)$ to vary from run to run²⁵ and represent the spontaneous break-

ing of continuous translational symmetry in the system. This result therefore represents the first steps toward realizing novel, controllable condensed matter systems involving phase transitions via emergent structure.^{6,7,13}

The temporal intensity profile of the generated light provides additional insight into the evolution of the instability. Figure 2b shows $I_{s,i}(t)$, where we turn on the pump beams at $t = 0$. As the atoms cool and organize in the presence of the pump beams, the signal and idler intensities grow exponentially and reach a maximum value I_{peak} after a time τ_D . Stronger pumping reduces τ_D , which is typically on the order of 10's of μs . The generated fields, which can be as large as $0.2I_p$, act back on the vapor and strongly affect the ensuing dynamics. The details of the long-term behavior therefore vary from run to run, but typically consist of additional bursts of light with characteristic durations on the order of 10 – 100 μs due to atomic motion in the underlying optical lattice.

The signal and idler fields display strong temporal correlations due to their mutual coupling, where the cross-correlation coefficient $r_{s,i}(0)$ is typically greater than 0.9 (see Methods). The correlations arise because the generated fields are coupled via the density grating, in contrast to experiments carried out using standing-wave cavities where the mirror boundary conditions necessarily impose correlations. While we have only measured the classical correlations between the signal and idler beams, we anticipate that quantum correlations also exist and make this system useful for twin beam generation.²⁶

After a few hundred μs , expansion of the cloud along the unconfined \hat{y} direction reduces the

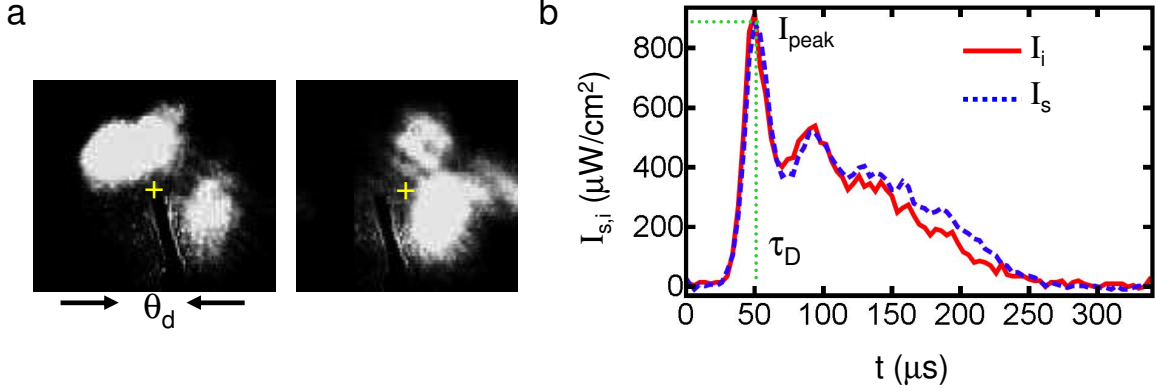


Figure 2: **Multi-mode and temporally-correlated superradiant emission.** **a**, The left and right images show $I_s(x, y)$ in the far field for two experimental MOT realizations, where the center of the image (indicated by a +) corresponds to light propagating along the \hat{z} -direction. The generated light consists of multiple spatial modes that vary from one run to the next. The angular width of each beam is $\theta_D = 3.1 \pm 0.4$ mrad, corresponding to a diffraction-limited beam waist ($1/e$ field radius) of 158 ± 20 μm at the exit of the trap. **b**, Temporal dependence of $I_{s,i}$ after we turn the pump beams on at $t = 0$. After a dwell time, the fields grow exponentially, reach a maximum value of I_{peak} at time τ_D , and display a high degree of correlation $r_{s,i}(0) = 0.987$. After several additional bursts, oscillation terminates by ~ 250 μs . We use $I_p = 4 \pm 0.1$ mW/cm^2 , $\Delta = -5 \pm 0.5$ Γ and $\eta = 5 \pm 2 \times 10^{10}$ cm^{-3} .

atomic density and superradiance ends. We overcome this expansion and maintain steady-state superradiance by keeping the MOT beams on at reduced intensities (typically 5 – 10% of their full values) during the application of the pump beams. The atoms can therefore continue to interact with the pump beams while remaining free to self-organize. This modified scheme enables us to realize superradiance that persists for up to several seconds (limited only by the timing electronics), although the amplitude of the generated light is smaller than in the absence of the MOT fields (see Fig. 3a). We use this long-term time series to calculate the degree of second-order coherence $g_{s,i}^{(2)}(\tau)$ (see Methods) and find that $g_{s,i}^{(2)}(0) = 1.125 \pm 0.05$, where $g^{(2)}(\tau) = 1$ for a coherent field (see Fig. 3b). Thus, the generated light is nearly coherent, which is consistent with recent predictions on steady-state superradiance.¹ In addition, the coherence time is typically several hundred μs , which is over 100 times larger than that observed for a cloud of unconfined atoms at comparable temperatures.²⁰

The unique properties of our system suggest a variety of future applications. For pump beams focused to an optical cross section (*i.e.*, $\lambda^2/2\pi$, where $\lambda = 780$ nm is the optical wavelength), we predict that we require only ~ 100 photons to drive the instability. This low threshold, combined with the system's long coherence time, indicates its potential as a quantum memory² or quantum logic element.²⁷ In addition, our system's capacity to support multiple spatial modes makes it an excellent candidate for studying continuous-variable quantum information protocols based on spatial multimode entanglement,^{8,9} low-light-level all-optical switching,^{20,28} and multidimensional optical soliton formation.²⁹ Finally, the self-phase-matching nature of the collective instability may provide a simple path toward the efficient generation of tunable short-wavelength light.³⁰

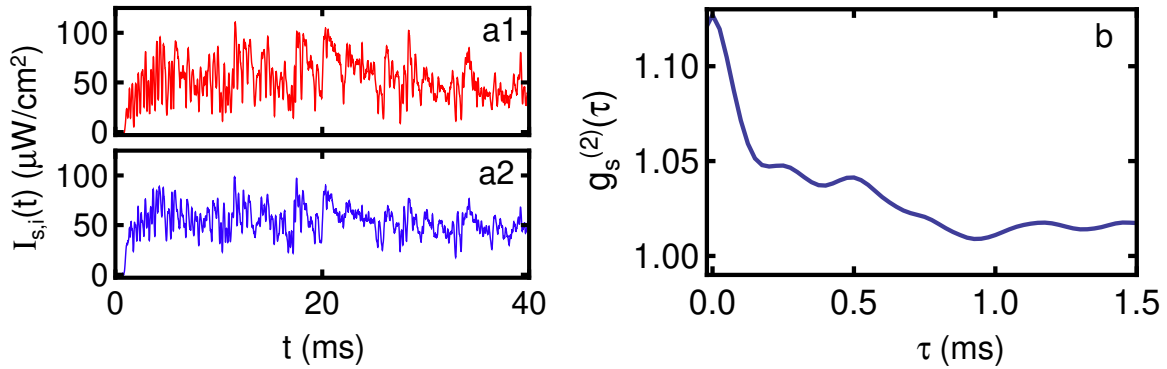


Figure 3: **Steady-state superradiance and its coherence properties.** Typical steady-state temporal waveform of the **a1**, idler and **a2**, signal intensities obtained when we leave the MOT beams on at a reduced intensity during the application of the pump beams. The signal and idler fields show strong correlations [$r_{s,i}(0) = 0.90$] for the duration of emission. **b**, The degree of second-order coherence $g_s^{(2)}(\tau)$ for the signal beam time series shown in **a1**. Here, $I_p = 4 \pm 0.1 \text{ mW/cm}^2$, $\Delta = -5 \pm 0.5 \Gamma$, and $\eta = 5 \pm 2 \times 10^{10} \text{ cm}^{-3}$.

Methods

Experimental methods. In our experiment, we use an anisotropic magneto-optical trap (MOT) to confine ^{87}Rb atoms in a cylindrical region with a length $L = 3$ cm and $1/e$ diameter $W = 430$ μm .¹⁸ This corresponds to a Fresnel number $F = \pi W^2/(\lambda L) \cong 6$. We obtain typical atomic temperatures $T = 30$ μK and densities $\eta = 5 \times 10^{10}$ cm^{-3} , which leads to an on-resonant optical depth of $OD > 60$ ($OD \sim 1$) along the \hat{z} - (\hat{x} - and \hat{y} -) direction(s). We tune the intensity-balanced pump beams below the $5S_{1/2}(F = 2) \rightarrow 5P_{3/2}(F' = 3)$ atomic transition by $|\Delta| = 2 - 20$ Γ , where $\Gamma/2\pi = 6$ MHz. We use wave plates and polarizers to independently set the polarizations of the pump beams, and find that superradiance occurs for linearly cross-polarized, linearly co-polarized, and circular co-rotating pump beam polarizations. We control the amplitudes of all externally-applied optical fields with acousto-optic modulators with response times of < 100 ns.

We cycle between a cooling and trapping period (where only the MOT beams are on) and a superradiant period (where the pump beams are on).²⁰ During the superradiant period, we either reduce or extinguish the intensity of the MOT beams. When we turn the MOT beams off, we use a 99 ms cooling and trapping period and a 1 ms superradiant period. When we leave the MOT beams on at a reduced intensity, we use a 99 ms cooling and trapping period followed by a superradiant period of variable length (up to 5 seconds). We leave the MOT repump beams and magnetic fields on to ensure that atoms are not pumped into a dark state and to enable continuous cooling and trapping, respectively. We have verified that the MOT magnetic fields do not affect the superradiance when the MOT beams are off.²⁰

We measure the time- and space-dependent signal and idler intensities using a pair of matched, large-area photo multiplier tubes (PMTs, Hamamatsu H-6780) and a fast charge-coupled device (CCD) camera (Dalsa), respectively. We place a 200 mm lens in the path of the signal beam 33 cm beyond the end of the trap (after the beam splitter) and position the CCD camera 35 cm from the lens. We therefore image the far field such that the images represent the angular distribution of the emitted light.

Analysis of superradiance. We determine I_{thresh} by recording the dependence of $I_{s,i}$ on I_p (as shown in Fig. 1b) and fit a straight line to the data immediately after $I_{s,i}$ becomes distinguishable from detector noise. We define I_{thresh} as the value of I_p at which this line intersects the horizontal axis. The error in this fit constitutes the dominant contribution to the uncertainty in I_{thresh} . In contrast, the uncertainty associated with the beam waist of the generated optical fields represents the shot-to-shot variation between the emitted beams. All uncertainties correspond to one standard deviation.

We analyze the similarity between the signal and idler fields using the temporal cross correlation function $r_{s,i}(\tau) = \langle (I_s(t) - \bar{I}_s)(I_i(t + \tau) - \bar{I}_i) \rangle / (\overline{I_s^2 I_i^2})^{1/2}$, where $\langle \dots \rangle$ represents a time average and $\bar{A} \equiv \langle A \rangle$. To study the coherence properties of the generated optical fields, we calculate the degree of second order coherence $g_j^{(2)}(\tau) = \langle I_j(t) I_j(t + \tau) \rangle / \overline{I_j(t)^2}$, where $j = \{s, i\}$. For a coherent field, $g^{(2)}(\tau) = 1$.

1. D. Meiser and M. J. Holland. Intensity fluctuations in steady-state superradiance. *Phys. Rev. A* **81**, 063827 (2010).

2. J. Simon, H. Tanji, S. Ghosh, and V. Vuletic. Single-photon bus connecting spin-wave quantum memories. *Nat. Phys.* **3**, 765–769 (2007).
3. M. Saffman and Y. Wang. Collective focusing and modulational instability of light and cold atoms. In *Dissipative Solitons: From Optics to Biology and Medicine*, vol. 751 of *Lecture Notes in Physics*, 361–380 (Springer Berlin / Heidelberg, 2008).
4. A. Schilke, C. Zimmermann, P. Courteille, and W. Guerin. Optical parametric oscillation with distributed feedback in cold atoms. *Nat. Photon.* **advance online publication** (2011).
5. S. Slama, G. Krenz, S. Bux, C. Zimmermann, and P. W. Courteille. Cavity-enhanced superradiant Rayleigh scattering with ultracold and Bose-Einstein condensed atoms. *Phys. Rev. A* **75**, 063620 (2007).
6. S. Gopalakrishnan, B. L. Lev, and P. M. Goldbart. Frustration and glassiness in spin models with cavity-mediated interactions. *Phys. Rev. Lett.* **107**, 277201 (2011).
7. P. Strack and S. Sachdev. Dicke quantum spin glass of atoms and photons. *Phys. Rev. Lett.* **107**, 277202 (2011).
8. M. Lassen, G. Leuchs, and U. L. Andersen. Continuous variable entanglement and squeezing of orbital angular momentum states. *Phys. Rev. Lett.* **102**, 163602 (2009).
9. V. Boyer, A. M. Marino, R. C. Pooser, and P. D. Lett. Entangled images from four-wave mixing. *Science* **321**, 544–547 (2008).

10. We use the term superradiance in order to be consistent with the terminology commonly used in the literature, but the case of collective emission from an initially-incoherently prepared sample is more accurately called superfluorescence .
11. R. H. Dicke. Coherence in spontaneous radiation processes. *Phys. Rev.* **93**, 99–110 (1954).
12. K. Baumann, C. Guerlin, F. Brennecke, and T. Esslinger. Dicke quantum phase transition with a superfluid gas in an optical cavity. *Nature* **464**, 1301 – 1306 (2010).
13. D. Nagy, G. Kónya, G. Szirmai, and P. Domokos. Dicke-model phase transition in the quantum motion of a Bose-Einstein condensate in an optical cavity. *Phys. Rev. Lett.* **104**, 130401 (2010).
14. S. Inouye, A. P. Chikkatur, D. M. Stamper-Kurn, J. Stenger, D. E. Pritchard, and W. Ketterle. Superradiant Rayleigh scattering from a Bose-Einstein condensate. *Science* **285**, 571–574 (1999).
15. Y. Yoshikawa, Y. Torii, and T. Kuga. Superradiant light scattering from thermal atomic vapors. *Phys. Rev. Lett.* **94**, 083602 (2005).
16. C. von Cube, S. Slama, D. Kruse, C. Zimmermann, P. W. Courteille, G. R. M. Robb, N. Piovella, Bonifacio, and R. Self-synchronization and dissipation-induced threshold in collective atomic recoil lasing. *Phys. Rev. Lett.* **93**, 083601 (2004).
17. A. T. Black, H. W. Chan, and V. Vuletić. Observation of collective friction forces due to spatial self-organization of atoms: From Rayleigh to Bragg scattering. *Phys. Rev. Lett.* **91**, 203001 (2003).

18. J. A. Greenberg, M. Oriá, A. M. C. Dawes, and D. J. Gauthier. Absorption-induced trapping in an anisotropic magneto-optical trap. *Opt. Express* **15**, 17699–17708 (2007).
19. J. Dalibard and C. Cohen-Tannoudji. Laser cooling below the doppler limit by polarization gradients: simple theoretical models. *J. Opt. Soc. Am. B* **6**, 2023–2025 (1989).
20. J. A. Greenberg, B. L. Schmittberger, and D. J. Gauthier. Bunching-induced optical nonlinearity and instability in cold atoms [Invited]. *Opt. Express* **19**, 22535–22549 (2011).
21. J. A. Greenberg and D. J. Gauthier. High-order optical nonlinearity at low light levels. *ArXiv e-prints* (2011). 1108.4730.
22. One can also discuss this gain mechanism in terms of multi-wave mixing between the optical and matter fields. In this case, superradiance is identical to parametric self-oscillation, where the amplification of initial density and optical field fluctuations gives rise to macroscopic density gratings and emitted optical fields .
23. S. Inouye, R. F. Löw, S. Gupta, T. Pfau, A. Görlitz, T. L. Gustavson, D. E. Pritchard, and W. Ketterle. Amplification of light and atoms in a Bose-Einstein condensate. *Phys. Rev. Lett.* **85**, 4225 (2000).
24. A. S. Zibrov, M. D. Lukin, and M. O. Scully. Nondegenerate parametric self-oscillation via multiwave mixing in coherent atomic media. *Phys. Rev. Lett.* **83**, 4049–4052 (1999).
25. M. G. Moore and P. Meystre. Theory of superradiant scattering of laser light from Bose-Einstein condensates. *Phys. Rev. Lett.* **83**, 5202–5205 (1999).

26. M. Vallet, M. Pinard, and G. Grynberg. Generation of twin photon beams in a ring four-wave mixing oscillator. *EPL (Europhysics Letters)* **11**, 739–744 (1990).
27. H. J. Kimble. The quantum internet. *Nature* **453**, 1023–1030 (2008).
28. A. M. C. Dawes, D. J. Gauthier, S. Schumacher, N. H. Kwong, R. Binder, and A. Smirl. Transverse optical patterns for ultra-low-light-level-all-optical switching. *Laser and Photon. Rev.* **4**, 221–243 (2010).
29. G. Fibich, N. Gavish, and X. P. Wang. Singular ring solutions of critical and supercritical nonlinear Schrödinger equations. *Physica D* **231**, 55–86 (2007).
30. G. R. M. Robb and B. W. J. McNeil. Four-wave mixing with self-phase matching due to collective atomic recoil. *Phys. Rev. Lett.* **94**, 023901 (2005).

Acknowledgements We gratefully acknowledge the financial support of the NSF through Grant #PHY-0855399.

Author Contributions J.A.G. carried out the experiment and data analysis. J.A.G and D.J.G. conceived of the experiment, interpreted the data, and wrote the paper.

Competing Interests The authors declare that they have no competing financial interests.

Correspondence Correspondence and requests for materials should be addressed to J.A.G.